# Signal Distortion by Analog Filters in RF Front-End Circuits at Wireless Receivers

Xinzhe Pi[1], Meiyun Xie[1], Yu Zhang[2]
[1]School of Systems Information Science, Future University Hakodate, Hakodate, Hokkaido, 041-8655, Japan
[2]School of Computer Science and Technology, Xidian University, Xi'an, Shaanxi, 710071, China

**Radio frequency front-end (RFFE) circuit design significantly improves signal quality for demodulation and decoding in wireless receivers. Due to the diversity and complexity of circuit designs, as well as potential distortions to signals, there is no theoretical model to measure the impact of RFFE circuits on radio signals. To address this critical and challenging issue, we first focus on analog filters in RFFE circuits, which directly affect signal reception and carrier recovery, and consequently influence the demodulation error probability. In this paper, we discuss the role of analog filters in RFFE circuits and the model of their effect on signals. We also introduce different types of distortions caused by analog filters, which are related to signal amplitude, phase, and frequency. Based on these, we propose using the Wiener model to characterize the impact of analog filters on signals considering nonlinear distortions. This work may shed light on developing a feasible analytical model of how RFFE circuits influence demodulation errors at wireless receivers.**

***Index Terms*—Wireless communication, signal distortion, RFFE circuit, analog filter, nonlinear model.**

## I. Introduction

SINCE the advent of wireless communication technology, human society has undergone tremendous changes. To support high-speed and reliable communication, modulation technology has been proposed to utilize radio frequency (RF) signals (frequencies between 20KHz and 300GHz) that propagate better in the air. Different modulation schemes support different communication rates but have corresponding requirements for signal quality. When the signal received by the receiver is highly distorted, or the noise component is prominent, the probability of demodulation error will also increase, thereby decreasing the communication quality.

The radio frequency front-end (RF front-end, or RFFE) circuit is a core part of wireless systems, and it is located between the antenna and the digital baseband signal circuit. At wireless transmitters, RFFE circuits focus on delivering high-power signals with minimal distortion to meet transmission distance and spectral compliance requirements. At wireless receivers, RFFE circuits deal with signal amplification, filtering, and carrier recovery, which aim to improve signal quality and reduce demodulation errors. Generally, RFFE circuits consist of power amplifiers, analog filters, oscillators, and mixers.

Although many works have given more approximate expressions for the symbol error rate (SER) of different modulation schemes, these results are based on ideal signals and the basic Gaussian noise model [1], [2]. In fact, radio signals will experience significant attenuation and moderate distortion after passing through a wireless channel, including the impact of multipath fading, Doppler shifts, and noise, and RFFE circuits at receivers are designed to compensate for these effects.

For wireless channels, many mathematical models can simulate the impacts of various channels on the signal well, such as the Rayleigh fading channel and Rician fading channel, providing insights into signal amplitude and phase variations [3], [4], [5], [6], [7]. These models have been instrumental in analyzing the communication performance of different wireless systems and could be further applied to measure SER in demodulation. Recent studies have extended these models to account for complex channel environments, such as those encountered in high-frequency bands, where multipath effects and Doppler shifts become more pronounced [8].

Studies on electrical components such as power amplifiers, mixers, and oscillators have focused on nonlinearity and spurious signal generation, which can significantly degrade communication performance [9], [10], [11], [12], [13]. While the role of these components has been discussed, due to the diversity in design and the electromagnetic characteristics of various components, the impact of RFFE circuits on signals has also been discussed. For instance, adaptive filtering techniques have been proposed to address signal distortion dynamically, offering a promising direction for improving RFFE performance in real-time environments [14], [15]. However, the mathematical relationship between RFFE circuits and communication performance, especially the demodulation error probability, has not been studied and needs further discussion. Therefore, to accurately characterize the SER of modulation schemes, it is very important to establish a mathematical model of RFFE circuits for their impact on signals.

To address this challenging issue, we can divide it into multiple sub-problems and solve them individually. As an important part of the RF front-end circuit, the analog filter is responsible for filtering out-of-band noise and interference to acquire the expected signals from transmitters. However, analog filters could also introduce linear and nonlinear distortions and accordingly deteriorate signal quality, thereby affecting the SER of the system [16], [17]. In [18], Mehler et al. introduced a simplified approach to analyzing amplitude distortion in linear-phase filters. It focused on deriving approximate solutions for passband variations, and the proposed

Manuscript received December 16, 2024; revised January 15, 2025. Corresponding author: Xinzhe Pi (email: pxinzhe@163.com).

method reduced computational complexity and guided early filter optimizations. However, this study does not consider nonlinear distortions. In [19], Del Vecchio et al. presented an analytical methodology to estimate distortion in continuous-time filters. They employed small-signal approximations to assess filter-based nonlinearity, and this approach enabled designers to detect potential issues early in the circuit design phase. While addressing certain distortion aspects, this paper does not comprehensively model nonlinear distortions, such as those arising from component nonlinearity or high-power signal interactions. In [20], Ismail et al. proposed an approximate distortion analysis dedicated to active-RC filters. They investigated how component-level nonlinearity accumulates within the filter's transfer function. External factors like temperature variations, power supply noise, or component aging are not considered in this work, which can affect the accuracy and reliability of the distortion models in practical settings.

Although the results in [18], [19], [20] offered practical guidelines for achieving low-distortion circuit implementations, these works still have their limitations, as stated above. Therefore, it is of great significance to further study the impact of analog filters on system performance with linear and nonlinear distortions. The primary contribution of this study is that we analyze the impact of linear and nonlinear distortions on signals introduced by analog filers and propose using the Wiener model to build a mathematical model considering both types of distortions, which may shed light on developing a feasible analytical model of how RFFE circuits influence demodulation errors at wireless receivers.

The rest of this paper is organized as follows. Section II introduces analog filters in RFFE circuits and the system function of filters as their system models. In Section III, we discuss distortions potentially caused by analog filters and their relations to system functions. Then, in Section IV, we propose using the Wiener model to obtain a mathematical model of analog filters considering nonlinear distortions. Finally, Section V concludes the paper and discusses our future work.

## II. Linear Model of Analog Filters

In this section, we first introduce the role of analog filters within a wireless RFFE circuit, illustrating what band-pass filters (BPFs) and low-pass filters (LPFs) do in a direct conversion receiver. Next, we describe the impulse response, frequency response, and system function of linear time-invariant (LTI) filters, highlighting their relevance to wireless signals. Finally, we discuss the design procedure for analog filters and how the transfer function $H(s)$ is determined.

### A. Analog Filters in Wireless RF Front-End Circuit

In wireless communications, there are different kinds of transceiver circuit architectures, such as superheterodyne, direct conversion, low intermediate frequency (IF), etc. Different architectures exhibit their advantages and disadvantages, and employ diverse signal processing, including filtering. Consequently, different architectures require varying numbers and types of filters. The direct conversion architecture, also known as zero-IF, is currently the most widely used in wireless communication systems.

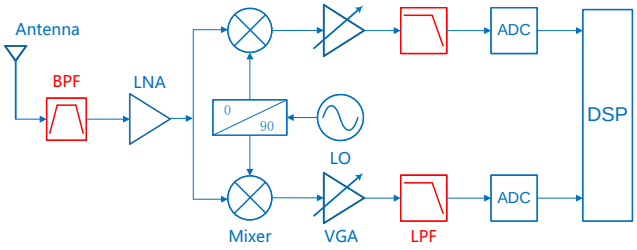


Fig. 1: Diagram of the direct conversion architecture.

The diagram of direct conversion architecture is shown in Fig.1, and it is a wireless receiver circuit diagram using IQ (in-phase and quadrature) modulation. The antenna receives RF signals from the propagation media, and we first use a BPF to get the signals within the concerned frequency band and eliminate unexpected out-of-band noise and interference. The filtered RF signal is then amplified by the low-noise amplifier (LNA) to boost the signal strength without significantly degrading the signal-to-noise ratio (SNR).

Next, the amplified RF signal is mixed with a local oscillator (LO) signal. In a zero-IF architecture, the LO frequency is set equal to the RF signal frequency. This results in the direct conversion of the RF signal to the baseband. The mixing process generates two outputs: the in-phase and quadrature components of the baseband signal, typically achieved by mixing RF signals with two LO signals that are 90 degrees out of phase.

The baseband I and Q signals (in-phase and quadrature components) are further amplified using variable gain amplifiers (VGA). VGAs adjust the signal amplitude dynamically to match the optimal range of the analog-to-digital converter (ADC). Since the mixing process could generate a high-frequency component named mirror interference, an LPF is needed to eliminate it and retain only the baseband signal. Then, ADCs digitize the amplified and filtered analog I and Q signals, and digitized signals undergo signal processing depending on the specific communication protocol or application, such as filtering, demodulation, and error correction.

According to the signal processing procedure above, we can find that the BPFs and LPFs play significant roles in wireless transceiver circuits.

### B. Response Functions of Analog Filters

The objective of filters is to retain the signal in the desired frequency band and filter out the signal at other frequencies. Therefore, an ideal filter is a linear time-invariant (LTI) system.

**LTI System:** An LTI system means that the system produces an output signal from any input signal subject to the constraints of **linearity** and **time-invariance**.

**Linearity:** The filter output is linearly related to the input signal, satisfying the superposition principle. It means that if the input signal is a linear combination of multiple signals, the output will also be a linear combination of these signals after passing through the filter.

**Time-invariance:** The characteristics of a filter do not change over time. That is, the filter's response is the same regardless of when the input signal is applied.

Suppose the continuous-time input signal of a filter is $x(t)$. The output signal $y(t)$ can be represented as

$$y(t) = x(t) * h(t) + n(t), \tag{1}$$

where $h(t)$ is the **impulse response** of the filter and $n(t)$ is the additive noise introduced by the filter. Here, $*$ denotes the convolution operation and $x(t)*h(t) = \int_{-\infty}^{+\infty} x(\tau)h(t-\tau)d\tau$.

Since a filter processes the input signal in the frequency domain, we are more concerned with its **frequency response** $H(f)$. We can obtain the frequency response by $H(f) = \mathcal{F}\{h(t)\}$, where $\mathcal{F}$ denotes the Fourier transform and $\mathcal{F}\{h(t)\} = \int_{-\infty}^{+\infty} h(t)e^{-j2\pi ft}dt$. Then, the spectrum of $y(t)$ can be obtained by

$$Y(f) = X(f)H(f) + N(f), \tag{2}$$

where $X(f)$ and $N(f)$ are the spectrum of $x(t)$ and $n(t)$, respectively.

Considering the frequency response in the complex frequency domain, we can get the **system function** $H(s)$, also known as the transfer function, by setting $s = \sigma + j2\pi f$. In this case, $H(s) = \int_{-\infty}^{+\infty} h(t)e^{-st}dt$, where $\mathcal{L}$ denotes the Laplace transform. Notice that $H(s)$ contains the pole and zero information of the system, which can be used for filter design.

### C. System Function in Analog Filter Design

From Section II-B, we can calculate the output of a filter if we know the input and the system function (or impulse response or frequency response). Generally, we can determine $H(s)$ while designing the filter circuit diagram. For example, we can follow the steps below to design an analog band-pass filter.

**Step 1:** Confirm the center frequency $f_0$ and the bandwidth $\Delta f$. The center frequency is usually the same as the carrier frequency;

**Step 2:** Select the topology type and order of filters. Different topology types perform differently in the passband, stopband, and skirt. For example, a Butterworth filter is recommended when we need a flat passband response. The order represents the complexity of the filter circuit, and a higher order achieves a steep skirt, which means a better frequency selectivity;

**Step 3:** Select the parameters of electronic components (like capacitors and inductors) based on $H(s)$. Notice that when $n$ is even, a $n$th-order band-pass filter consists of $n/2$ 2-order band-pass filters. Thus the overall system function $H(s)$ with the order $n$ can be represented as

$$H(s) = \begin{cases} K\prod_{k=1}^{n/2} \frac{\Delta\omega_k s}{s^2+\Delta\omega_k s+\omega_k^2}, & \text{even } n, \\ K\prod_{k=1}^{(n-1)/2} \frac{\Delta\omega_k s}{s^2+\Delta\omega_k s+\omega_k^2} \cdot \frac{a_1 s+a_0}{s+\omega_c}, & \text{odd } n, n \geq 3. \end{cases} \tag{3}$$

$K$ denotes the overall gain coefficient of the $n$th-order filter. $f_k = 2\pi f_k$ and $\Delta f_k$ represent the center frequency and bandwidth of $k$-th 2nd-order band-pass filter, respectively. In (3), $\omega_k = 2\pi f_k$ and $\Delta\omega_k = 2\pi\Delta f_k$. An odd-order band-pass filter has a cascade structure that consists of $(n-1)/2$ 2-order band-pass filters and a 1st-order low-pass or high-pass filter. If the 1st-order filter is a low pass filter, $a_1 = 0$ and $a_0$ is a constant. Otherwise, if it is a high pass filter, $a_0 = 0$ and $a_1$ is a constant. An odd-order band-pass filter can achieve a wider passband and a smoother response, while an even-order one provides a steeper skirt and better frequency selectivity.

Additionally, the design of other kinds of analog filters, such as a low-pass filter, is similar to the upper process. After we decide on the filter topology and order, we can obtain the component parameters in filter circuits based on the corresponding $H(s)$ and available parameter tables. Therefore, we can get the system function $H(s)$ from the filter circuit diagram in reverse and further analyze the mathematical features of the filter.

## III. Signal Distortions by Analog Filters

This section focuses on various types of signal distortions introduced by analog filters. We first examine amplitude and phase distortions, which are often inevitable due to non-ideal frequency responses. Then, we address nonlinear distortions that can arise under high-level inputs or from parasitic components. Finally, we discuss noise-related effects that further degrade signal quality, emphasizing thermal noise, flicker noise, electromagnetic interference, and parasitic effects.

### A. Amplitude Distortion

When signal components of different frequencies pass through the filter, they may be attenuated or amplified differently. An ideal filter should maintain constant gain in the passband and achieve complete attenuation in the stopband, but it is often difficult for actual filters to achieve this.

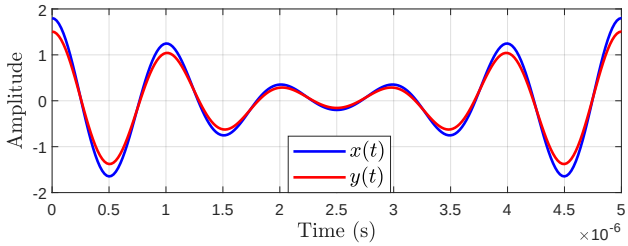


(a) Comparison of $x(t)$ and $y(t)$ considering only the amplitude distortion.

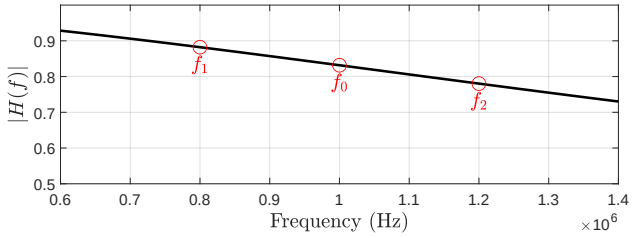


(b) Magnitude response of the filter with $H(s)$.

Fig. 2: Amplitude distortion.

**Amplitude distortion** (also called magnitude distortion) causes some frequency components of the signal to be amplified or attenuated unevenly, thereby changing the amplitude spectrum of the signal and causing the waveform to change. For a filter with frequency response $H(f)$, the amplitude response is expressed as

$$|H(f)| = \sqrt{(\mathrm{Re}\{H(f)\})^2 + (\mathrm{Im}\{H(f)\})^2}. \quad (4)$$

An ideal filter has an invariant $|H(f)|$ over the passband without amplitude distortion.

Fig.2 shows an example of amplitude distortion caused by a BPF. In Fig.2(a), the input signal is $x(t) = \cos 2\pi f_0 t + 0.5\cos 2\pi f_1 t$, where $f_0 = 1\mathrm{MHz}$ and $f_1 = 0.8\mathrm{MHz}$. $y(t)$ denotes the output signal through an LPF. The system function of the LPF is $H(s) = \frac{\omega_c}{s+\omega_c}$ where $\omega_c = 3\pi\mathrm{MHz}$. The corresponding magnitude response is shown in Fig.2(b). As we can see, the waveform of the output signal experiences an obvious amplitude distortion, which may result in demodulation errors.

### B. Phase Distortion

**Phase distortion** arises when the phase response of a filter is not linear with frequency. This nonlinearity can result in different frequency components experiencing different time delays, distorting the signal's waveform. Filters like Butterworth have non-linear phase responses, while Bessel filters are designed for linear phase to minimize phase distortion. For a filter with frequency response $H(f)$, the phase response is expressed as

$$\phi(f) = \arg[H(f)] = \arctan\frac{\mathrm{Im}\{H(f)\}}{\mathrm{Re}\{H(f)\}}. \quad (5)$$

An ideal filter has a phase response of $\phi(f) = -\alpha f + \phi_0$ without phase distortion.

Fig.3 shows an example of phase distortion. In 3(a), the input signal and system function are the same as those in Fig.2(a). Notice that we only show the magnitude distortion of $x(t)$ in Fig.2(a), we also only show the phase distortion of $x(t)$ in 3(a). The corresponding phase response is shown in Fig.3(b). Such distortion will cause a nonlinear phase delay between different frequency components of the signal, destroying the relative phase relationship of the frequency components. This has a great adverse effect on communication systems that use modulation technology using phase information and orthogonal frequency division multiplexing (OFDM) technology.

### C. Non-linear Distortion

**Non-linear distortion** generates harmonics and intermodulation products, introducing frequencies not present in the original signal. The possible reasons for non-linear distortion are as follows:

(1) Exceeding the linear operating range of components (high-level signals or overload);

(2) Inherent material and structural nonlinearities;

(3) Parasitic parameters and frequency-dependent effects;

(4) Intermodulation due to multiple frequencies.

A passive filter could introduce amplitude distortion and phase distortion (also called linear distortion), but no non-linear distortion. However, capacitors and inductors in filters may cause non-linear distortion with high-level input. Besides, some components inherently possess nonlinear characteristics due to their materials under high-voltage or high-frequency conditions. Parasitic parameters, frequency-dependent effects, and intermodulation also exist in filter circuits.

In filter design, it is assumed that all components are linear, and nonlinear distortion is caused by unexpected factors. Therefore, we cannot establish a mathematical model for non-linear distortion in advance and often measure such distortion

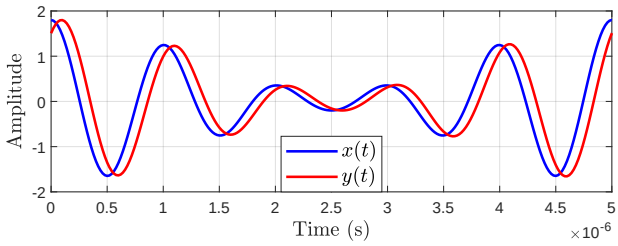


(a) Comparison of $x(t)$ and $y(t)$ considering only the phase distortion.

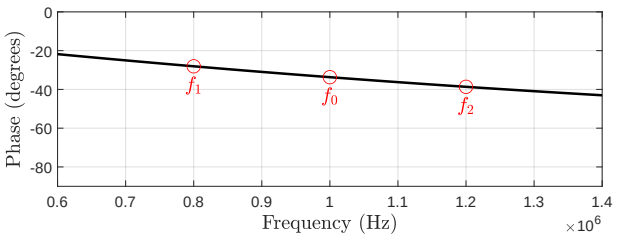


(b) Phase response of the filter with $H(s)$.

Fig. 3: Phase distortion.

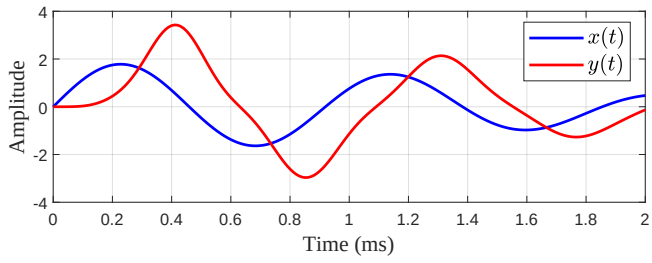


(a) Comparison of $x(t)$ and $y(t)$ in time domain.

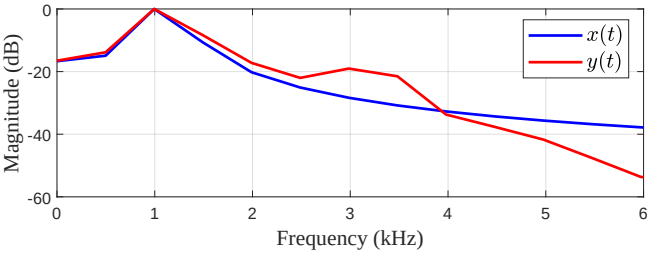


(b) Comparison of $x(t)$ and $y(t)$ in frequency domain.

Fig. 4: Nonlinear distortion.

TABLE I: Noise Types in Analog Filters

| **Noise Type** | **Origin** | **Model** | **Measurement Method** |
|---|---|---|---|
| Thermal Noise | Random electron motion | $V_{\text{rms}} = \sqrt{4kTRB}$ | Spectrum analyzer |
| Flicker Noise | Material imperfections | $S(f) \propto 1/f^{\alpha}$ | Low-frequency spectrum analysis |
| Electromagnetic Interference | External Electromagnetic fields | No universal model | Spectrum analyzer, shielding methods |
| Parasitic Effects | Unintended inductance/capacitance | $Z(f) = \frac{1}{j2\pi fC} + j2\pi fL$ | Impedance analyzer |

of circuits or components through testing. Common testing methods include single-tone test, We can judge the severity of distortion through the main performance indicators of nonlinear distortion, such as total harmonic distortion (THD) and third-order intercept point (IP3).

*1) Total Harmonic Distortion*

THD quantifies the extent of harmonic distortion present in a signal after it has passed through a system or component, such as an analog filter or amplifier. It is an indicator of the linearity of a system. To measure THD, a single-tone sinusoidal signal is input into the device, and a spectrum analyzer is used to capture and quantify the amplitudes of the fundamental and harmonic frequencies. The THD is then calculated by comparing the sum of the harmonic powers to the power of the fundamental tone, that is,

$$\text{THD} = \frac{\sqrt{V_2^2 + V_3^2 + V_4^2 + \cdots}}{V_1} \times 100\%, \tag{6}$$

where $V_1$ is the RMS voltage of the fundamental frequency, and $V_n$ is the RMS voltage of the $n$-th harmonic frequency. THD below 3% is often required to ensure signal integrity and reduce error rates in communication systems, and high THD values indicate significant distortion, which can degrade signal quality and impair system performance.

*2) Third-order Intercept Point*

IP3 is a theoretical point in the input power level where the power of the third-order intermodulation products equals the power of the fundamental tones. It serves as a measure of a system's linearity and its ability to handle multiple signals without generating significant intermodulation distortion. IP3 is measured by inputting two closely spaced sinusoidal tones into the device and using a spectrum analyzer to detect the resulting intermodulation products. By gradually increasing the input power and extrapolating the linear trends of the fundamental and intermodulation signals, the IP3 is determined as the hypothetical input power level where the intermodulation products would equal the fundamental tones. We can calculate it by

$$\text{IP3} = P_{\text{fund}} + \frac{P_{\text{IM3}} - P_{\text{fund}}}{2}, \tag{7}$$

where $P_{\text{fund}}$ is the power of the fundamental tones and $P_{\text{IM3}}$ is the power of third-order intermodulation products. Depending on the application and frequency band, IP3 values ranging from +10 dBm to +20 dBm are common in wireless communication systems, and a higher IP3 indicates better linearity.

An example of nonlinear distortion is shown in Fig.4. The input signal is $x(t) = \sin 2\pi \times 1000t + 0.8 \sin 2\pi \times 1200t$ and the system function of the filter is $H(s) = ((1 + \sqrt{2}s/\omega_c + s^2/\omega_c^2)(1 + s/\omega_c + s^2/\omega_c^2))^{-1}$ where $\omega_c = 5\pi$kHz. The nonlinear distortion is modeled as $f(x(t)) = x(t) + 0.3(x(t))^3$.

### D. Noise

In electronic filters, various types of noise can significantly influence the performance of signal processing. These noise sources arise from the inherent properties of components and external factors. The origins, mathematical models, and measurement methods of the major noise sources are briefly listed in Table I. Generally, we always consider the impact of thermal noise on signals. The existence and influence of other noises should be verified by testing. By studying these noise sources and their impacts, we can better design filters for specific applications and reduce noise-related performance degradation.

*1) Thermal Noise*

Thermal noise, also known as Johnson-Nyquist noise, originates from the random motion of electrons within a resistive material. Its power spectral density is uniform across frequencies (white noise), and it is described by the following equation:

$$V_{\text{rms}} = \sqrt{4kTRB}, \tag{8}$$

where $k$ is Boltzmann's constant ($1.38 \times 10^{-23}$ J/K), $T$ is the absolute temperature in Kelvin, $R$ is the resistance in ohms, and $B$ is the bandwidth in Hz.

Thermal noise can be measured using a spectrum analyzer by isolating the resistive component and observing the noise power across a given bandwidth. Careful calibration is essential to ensure that the measurement excludes external noise sources.

*2) Flicker Noise*

Flicker noise, or $1/f$ noise, arises from material imperfections and irregularities in the conduction process. Its power spectral density decreases with frequency and is generally modeled as:

$$S(f) \propto \frac{1}{f^{\alpha}}, \quad \alpha \approx 1, \tag{9}$$

where $f$ is the frequency and $\alpha$ is a material-dependent constant. This noise type dominates at low frequencies and is especially relevant in active components such as transistors. To measure flicker noise, low-frequency spectrum analysis is employed, focusing on frequencies where the noise dominates thermal noise.

*3) Electromagnetic Interference*

Electromagnetic interference (EMI) is caused by external electromagnetic fields coupling into the circuit. Unlike other noise types, EMI does not have a universal mathematical model due to its dependency on environmental factors and

coupling mechanisms. Measurement of EMI typically uses a spectrum analyzer to detect unintended signal peaks within the operating frequency range. Shielding and proper grounding are commonly used to mitigate EMI effects.

*4) Parasitic Effects*

Parasitic noise stems from unintended inductances, capacitances, or resistances within the circuit. These effects are particularly prevalent in high-frequency designs, where component and layout parasitics influence the circuit performance. The impedance of parasitic components is described as:

$$Z(f) = \frac{1}{j2\pi fC} + j2\pi fL, \tag{10}$$

where $C$ and $L$ represent parasitic capacitance and inductance, respectively. These parameters can be analyzed using an impedance analyzer to determine their frequency-dependent characteristics.

## IV. Nonlinear Model of Analog Filters with Distortions

Analog filters, which are often composed of passive components such as resistors, inductors, and capacitors, are regarded as LTI systems under small-signal conditions. For an ideal linear filter, given an input signal and the impulse response, the output signal and its spectrum can be calculated by convolution, as we state in Section II-A.

However, filters may exhibit nonlinear characteristics. For instance, nonlinearities in capacitors and inductors, saturation effects, or intermodulation distortions could break the linear assumption. In such scenarios, the output-input relationship cannot be described by linear convolution. Thus, circuit measurements and parameter estimation are necessary to characterize the output signals of nonlinear systems. Specifically, by applying well-defined test signals to the filter and measuring the output, one can obtain input-output data pairs. The challenge is then to select an appropriate modeling framework to represent the nonlinear system.

There are various approaches to modeling nonlinear systems. There are two basic models named the Hammerstein and Wiener models [21] [22] [23] [24], both of which decompose the system into distinct linear and nonlinear components. Passive analog filters are largely linear under small-signal conditions. However, non-ideal components in filters can introduce nonlinearities at higher signal levels. Such nonlinear effects are more naturally captured by the Wiener models. The model with input signal $x(t)$ and output signal $y(t)$ can be express by

$$w(t) = (h * x)(t), \tag{11}$$

$$y(t) = f(w(t)). \tag{12}$$

$x(t)$ is initially shaped by the linear filter and then passed through a nonlinear mapping $f(\cdot)$.

The linear response $h(t)$ of the filter can be approximately determined by the system function. Once $h(t)$ is known, deviations of the measured output from the linear prediction at larger input amplitudes can be attributed to the nonlinear function $f(\cdot)$ that follows the linear filter stage. To obtain the Wiener model, the parameters of $f(\cdot)$ must be determined. Using the known linear filter $h(t)$, we can compute the intermediate signal $w(t)$ by (11). This allows us to form data pairs $(w(t), y(t))$ by testing, which can be used to fit $f(\cdot)$. The relation between them can be modeled by a polynomial regression as

$$f(w(t)) = a_0 + a_1 w(t) + a_2 (w(t))^2 + \cdots . \tag{13}$$

The relation can also be modeled by other nonlinear fitting functions, such as saturation functions or piecewise linear segments. By minimizing the error between the measured $y(t)$ and the modeled $f(w(t))$, we can estimate the parameters of the nonlinear module. These procedures enable the development of a more accurate model of analog filters under non-ideal conditions, enhancing the accuracy of our analysis on signal processing and reducing demodulation errors.

## V. Simulation Result

In this section, we design an experiment to verify the effectiveness of the Wiener model in approximating the signal model of analog filters. A second-order Butterworth BPF is employed to simulate the linear characteristics of an RF passive filter. The filter is designed with the following parameters:

- Center Frequency: 1 GHz
- Bandwidth: 100 MHz
- Order: 2

The transfer function $H(s)$ of this BPF can be obtained based on these parameters and (3). The filter is implemented using `butter` function with normalized frequency specifications to accommodate a sampling rate of 10 GHz in MATLAB R2021b.

To emulate nonlinear distortions inherent in the BPF, a quadratic nonlinear term is introduced to the filter's output. The nonlinear filter model is defined as $y_{\text{real}}(t) = y(t) + n(t)$ and $y(t) = y(t) + \alpha \cdot (y(t))^2 + n(t)$, where:

- $y(t)$ is the nonlinear output signal,
- $H(s)$ represents the linear BPF transfer function
- $x(t)$ is the input signal
- $\alpha = 0.1$ is the nonlinear distortion coefficient
- $n(t) \sim \mathcal{N}(0, \sigma^2)$ is the AWGN noise signal and $\sigma = 0.05$

To simulate realistic wireless communication scenarios, Quadrature Amplitude Modulation (QAM) signals are generated as input. The specifics of the QAM signal generation are as follows:

- Modulation Order: 64
- Number of Symbols: 1000
- Carrier Frequency: 1 GHz

The symbols are generated using `qammod` function with unit average power normalization to ensure consistent signal amplitude. Each symbol is mapped to a corresponding in-phase and quadrature component, which are then modulated onto a 1 GHz carrier using cosine and sine functions, as $x(t) = \text{Re}\{s(t)\} \cdot \cos(2\pi f_c t) - \text{Im}\{s(t)\} \cdot \sin(2\pi f_c t)$, where $s(t)$ represents the complex QAM symbols.

The Wiener model capturing both the linear and nonlinear distortions is modeled as $y_{\text{pred}}(t) = y(t) + p_2 (y(t))^2 + p_1 y(t) + p_0$ where $p_2$, $p_1$, and $p_0$ are the polynomial coefficients

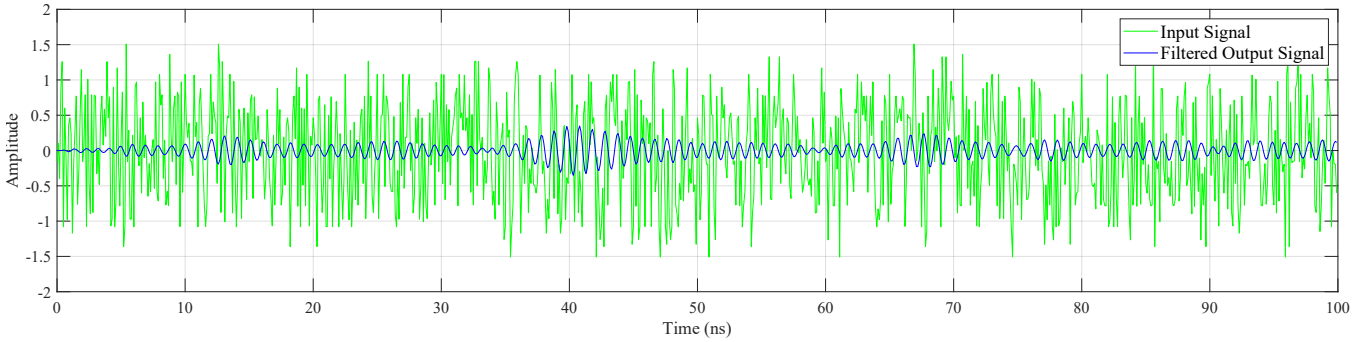


(a) Comparison of $x(t)$ and $y(t)$.

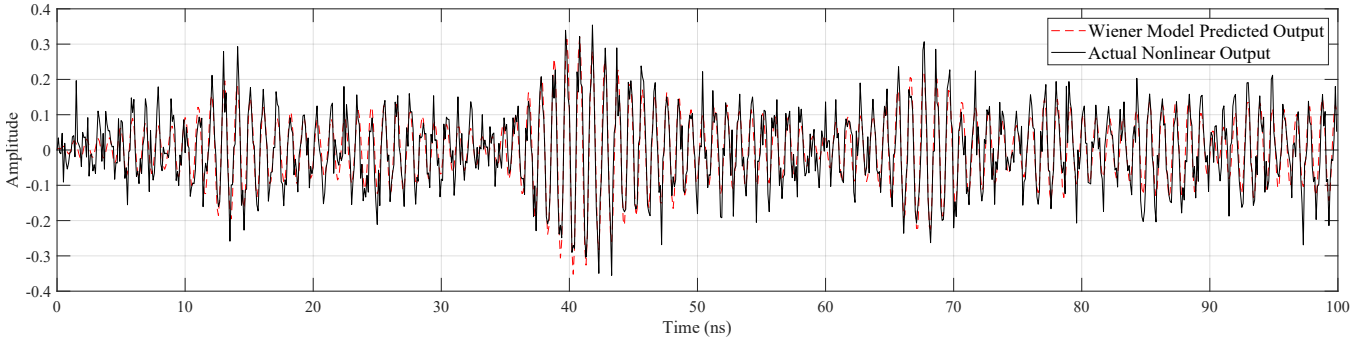


(b) Comparison of $y_{\text{real}}(t)$ and $y_{\text{pred}}(t)$.

Fig. 5: Simulation result.

determined through regression analysis using MATLAB's `polyfit` function.

We perform the experiment as follows:

(1) Randomly select multiple symbol signals from the set of all available symbols in QAM;

(2) Input these signals into the designed BPF and get the output signals;

(3) Using the data of output signals to fit the parameters of the Wiener model;

(4) Randomly select several symbol signals as the input of the BPF and Wiener model and compare the output signals $y_{\text{real}}(t)$ and $y_{\text{pred}}(t)$;

(5) Evaluate the error of the Wiener model.

By the procedure, we get the fitted model as $y_{\text{pred}}(t) = y(t) - 0.1553 \times (y(t))^2 + 0.96093 \times (y(t)) + 0.0043811$. Then, when a new signal is input, we compare the output signal of the BPF and the predicted signal of the Wiener model in Fig.5. From Fig.5-a, we can see that the BPF successfully filters the noise signal and outputs the QAM signals. From Fig.5-b, we can see that the output signal predicted by the fitted Wiener model is very similar to the signal output by the BPF. The mean square error calculated for the sampling points in the signal is 0.002455, which is acceptable. However, we also notice that the parameters of the fitted model are different from the parameters we set in the simulation. This may be due to the equivalence between different high-order trigonometric functions, which makes the performance of the fitted model and the real model similar even if the parameters are different. We will discuss this phenomenon further in future research.

## VI. Conclusion and Future Work

It is very challenging to characterize the mathematical relation between the RFFE circuit and demodulation error probability in wireless communications. Regarding the whole circuit as a signal system consisting of multiple components and submodules, in this paper, we focus on analog filters and explore their impact on signals in RFFE circuits. We first introduce the role of analog filters in RFFE circuits and the system function decided by filter designs. Various potential distortions caused by the filters are also discussed to illustrate their impact on signals. Considering the model complexity and further application in the modeling of the RFFE circuit signal model, we propose using the Wiener model to build a mathematical model of analog filters considering nonlinear distortions. Referring to the application of the Wiener model in characterizing analog filters, we can further analyze the impact of other crucial components and submodules on signals in RFFE circuits and finally address the challenging issue of characterizing the mathematical relation. This relation potentially reveals novel methods in RFFE circuit design and communication reliability and security optimization.

## References

[1] C.-C. Hsieh and T.-M. Chang, "On the General BER Expression of One- and Two-Dimensional Amplitude Modulations," *IEEE Transactions on Communications*, vol. 48, no. 6, pp. 998–1007, 2000.

[2] M. K. Simon and M.-S. Alouini, "M-PSK and M-QAM BER Computation Using Signal-Space Concepts," *IEEE Transactions on Communications*, vol. 54, no. 5, pp. 767–772, 2006.

[3] W. C. Jakes, *Microwave Mobile Communications*. Wiley, 1994.

[4] A. Goldsmith, *Wireless Communications*. Cambridge University Press, 2005.

[5] T. K. Sarkar, Z. Ji, K. Kim, A. Medour, and M. Salazar-Palma, "A Survey of Various Propagation Models for Mobile Communication," *IEEE Antennas and Propagation Magazine*, vol. 45, no. 3, pp. 51–82, 2003.
[6] A. F. Molisch, *Wireless Communications*, 2nd ed. John Wiley & Sons, 2011.
[7] D. Tse and P. Viswanath, *Fundamentals of Wireless Communication*. Cambridge University Press, 2005.
[8] A. F. Molisch, "Ultrawideband Propagation Channels: Theory, Measurement, and Modeling," *IEEE Transactions on Vehicular Technology*, vol. 54, no. 5, pp. 1528–1545, 2005.
[9] K. Kundert and A. Sangiovanni-Vincentelli, "A Unified Approach to the Analysis of Linear Amplifier Distortion," *IEEE Transactions on Circuits and Systems I: Regular Papers*, vol. 46, no. 3, pp. 379–390, 1999.
[10] R. Chaudhuri and D. Sanyal, "Design of CMOS Low Noise Amplifiers for RF Applications," *IEEE Transactions on Circuits and Systems I: Regular Papers*, vol. 52, no. 3, pp. 640–649, 2005.
[11] D. R. Morgan, Z. Ma, J. Kim, M. G. Zierdt, and J. Pastalan, "A Generalized Memory Polynomial Model for Digital Predistortion of RF Power Amplifiers," *IEEE Transactions on Signal Processing*, vol. 54, no. 10, pp. 3852–3860, 2006.
[12] H. S. Lee, D. T. Ma, and T. Takahashi, "Nonlinear Analysis of Passive Mixers in CMOS Technology," *IEEE Transactions on Microwave Theory and Techniques*, vol. 66, no. 8, pp. 3615–3626, 2018.
[13] B. Razavi, "A Study of Phase Noise in CMOS Oscillators," *IEEE Journal of Solid-State Circuits*, vol. 31, no. 3, pp. 331–343, 1996.
[14] B. Widrow and S. D. Stearns, "Adaptive Signal Processing," *IEEE Transactions on Circuits and Systems I: Regular Papers*, vol. 44, no. 3, pp. 210–223, 1996.
[15] D. Bhattacharyya and K. S. Shanmugam, "Adaptive Filtering and Its Applications in Wireless Communications," *IEEE Access*, vol. 6, pp. 43 117–43 129, 2018.
[16] R. Schaumann, M. S. Ghausi, and K. R. Laker, *Design of Analog Filters*, 2nd ed. Oxford, UK: Oxford University Press, 2010.
[17] B. Razavi, *Design of Analog CMOS Integrated Circuits*. New York, NY, USA: McGraw-Hill, 2001.
[18] M. L. Mehler, "Approximate Analysis of Linear-Phase Filter Amplitude Distortion," *IEEE Transactions on Audio and Electroacoustics*, vol. 21, no. 6, pp. 599–606, Dec. 1973.
[19] P. Del Vecchio and A. Trifiletti, "Analytical Approach for the Distortion Analysis of Continuous-Time Filters," in *Proc. IEEE International Symposium on Circuits and Systems (ISCAS)*, May 2011, pp. 2133–2136.
[20] M. Ismail, M. Olken, and T. Fiez, "On the Approximate Distortion Analysis of Active-RC Filters," *IEEE Transactions on Circuits and Systems I: Fundamental Theory and Applications*, vol. 39, no. 10, pp. 789–799, Oct. 1992.
[21] A. Hammerstein, "Nichtlineare Integralgleichungen mit Anwendungen auf Einige Probleme der Funktionalanalysis," *Mathematische Annalen*, vol. 104, no. 1, pp. 746–768, 1930.
[22] N. Wiener, *Nonlinear Problems in Random Theory*. Cambridge, MA: MIT Press, 1958.
[23] M. Schetzen, *The Volterra and Wiener Theories of Nonlinear Systems*. New York: John Wiley & Sons, 1980.
[24] L. Ljung, *System Identification: Theory for the User*, 2nd ed. Upper Saddle River, NJ: Prentice Hall, 1999.